Derivation of a Closed-Form Approximate Expression for the Self-Capacitance of a Printed Circuit Board Trace

Hwan W. Shim and Todd H. Hubing

***Abstract*—The electric fields that couple traces on printed circuit boards to attached cables can generate common-mode currents that result in significant radiated emissions. Previous work has shown that these radiated emissions can be estimated based on the self-capacitances of the microstrip structures on a board [6]. In general, the determination of these self-capacitances must be done numerically using three-dimensional static modeling software. In this paper, an approximate closed-form expression for the self-capacitance of microstrip traces is derived. This expression can be used to estimate the voltage-driven common-mode emissions from boards with various microstrip trace geometries. The expression also provides insight relative to the microstrip parameters that have the greatest effect on radiated emissions.**

***Index Terms*—Absolute capacitance, radiated emissions, self-capacitance, voltage-driven radiation, wire antenna.**

I. Introduction

Common-mode currents induced on cables attached to printed circuit boards (PCBs) are a primary source of unintentional radiated emissions [1]. One source of these currents is the potential difference induced across the board by the time-varying magnetic fields. This source mechanism is often referred to as *current driven* because the magnetic field strengths are generally proportional to the signal currents on the board. Electric fields can also couple directly to attached cables and induce the common-mode current on the cables. In this case, the coupling is proportional to the signal voltage and to the mutual capacitance between the attached cable and the source. This is generally called a *voltage-driven* mechanism. These basic mechanisms are illustrated in Fig. 1. Although the current-driven mechanism has been studied by several researchers [1]–[5], less research has been done on the voltage-driven mechanism. Nevertheless, voltage-driven common-mode currents induced by the microstrip structures on a PCB can be strong enough to cause electronic devices to fail to meet radiated emissions requirements [6]. A simple wire antenna with an equivalent common-mode voltage source, as shown in Fig. 2, can be used to calculate the radiated emissions.

The amplitude of the equivalent common-mode voltage source $V_{\rm CM}$ is proportional to the self-capacitance of the PCB trace. This capacitance can generally be calculated using three-dimensional (3D) electrostatic modeling codes. In this article, the parameters affecting the self-capacitance of a trace are investigated, and a closed-form expression is derived. Using this expression, the radiated emissions due to the coupling between microstrip traces and cables can be estimated without requiring numerical simulations.

II. Effect of Dielectric on Self-Capacitance of a Trace

In practice, a PCB has a dielectric material that separates the signal traces from the return plane. The dielectric material changes the electric field distribution, which affects the self- and mutual capacitances of the trace and plane. Considering a typical geometry, e.g. Fig. 3, the differential-mode capacitance, $C_{\rm DM}$, strongly depends on the dielectric permittivity of the insulator because the electric fields are primarily coupled through the dielectric. The self-capacitance of the trace, however, is a relatively weak function of the dielectric because the corresponding fields exist primarily outside the dielectric. In this section, two-dimensional (2D) electrostatic field simulations are used to investigate the effects of the dielectric on the self-capacitance of a microstrip.

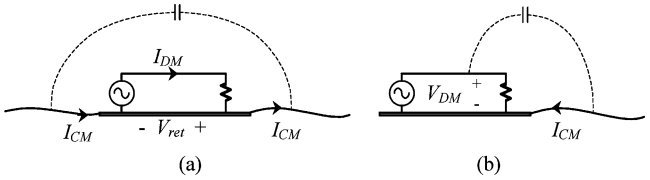

Fig. 1. Common-mode current mechanisms: (a) current-driven source and (b) voltage-driven source.

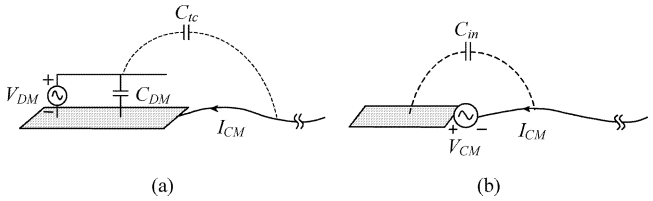

Fig. 2. Equivalent model of voltage-driven radiation mechanism.

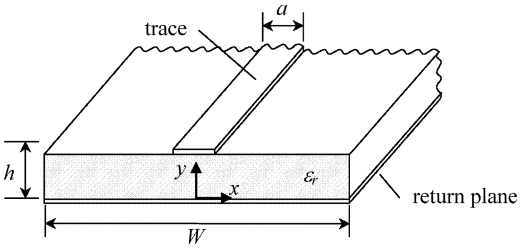

Fig. 3. Geometry of a microstrip trace with a finite-width return plane.

Assuming a quasi-TEM model, the field distribution of a microstrip structure can be obtained using a free-space Green's function formulation in terms of equivalent surface charge sources on the boundaries. A set of coupled integral equations in terms of the equivalent sources was formulated and enforced to satisfy the boundary conditions. The details can be found in the literature [7]–[9]. Using a technique based on this approach, the charge induced on various 2-D microstrip geometries was calculated.

The calculated induced charges for one example are shown in Fig. 4. The charges induced on each side of the conductors are illustrated separately. As expected, a significant portion of the charge is induced on the dielectric side of each conductor. The charge distribution on the trace is similar to that obtained for an infinitely wide return plane [13]. The charges on the reference plane, however, exhibit a peak near the edge due to the truncation of the plane. This peak is associated with the concentration of the electric fields at the edges. In general, the amount of charge on the dielectric side is greater than that on the opposite side.

The capacitances associated with the microstrip can be determined from the net charge on the trace and the plane when the potentials of the trace and plane are 1.0 and 0.0 V, respectively. The calculated capacitances as a function of dielectric permittivity are shown in Fig. 5. For a board with a plane width much greater than the separation between the trace and the plane, the differential-mode capacitance, $C_{\rm DM}$, is a function of the dielectric permittivity and the ratio of the trace width to

Manuscript received March 1, 2005; revised August 22, 2005.

H.-W. Shim is with the Mobile Communications Devision, Samsung Electronics Company, Gumi-city Gyeong-buk, Korea 730-350.

T. Hubing is with the Department of Electrical Engineering, University of Missouri, Rolla, MO 65409 USA (e-mail: hubing@umr.edu).

Digital Object Identifier 10.1109/TEMC.2005.859059

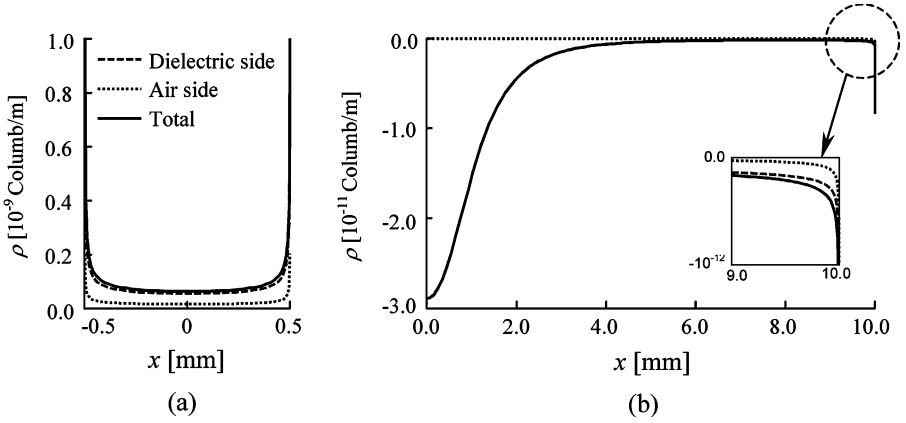

Fig. 4. Charge distribution on the trace (a) and plane (b), $W = 20.0$ mm, $a = h = 1.0$ mm, $\varepsilon_r = 4.0$, $V_{\text{trace}} = 1.0$ V, $V_{\text{plane}} = 0$ V.

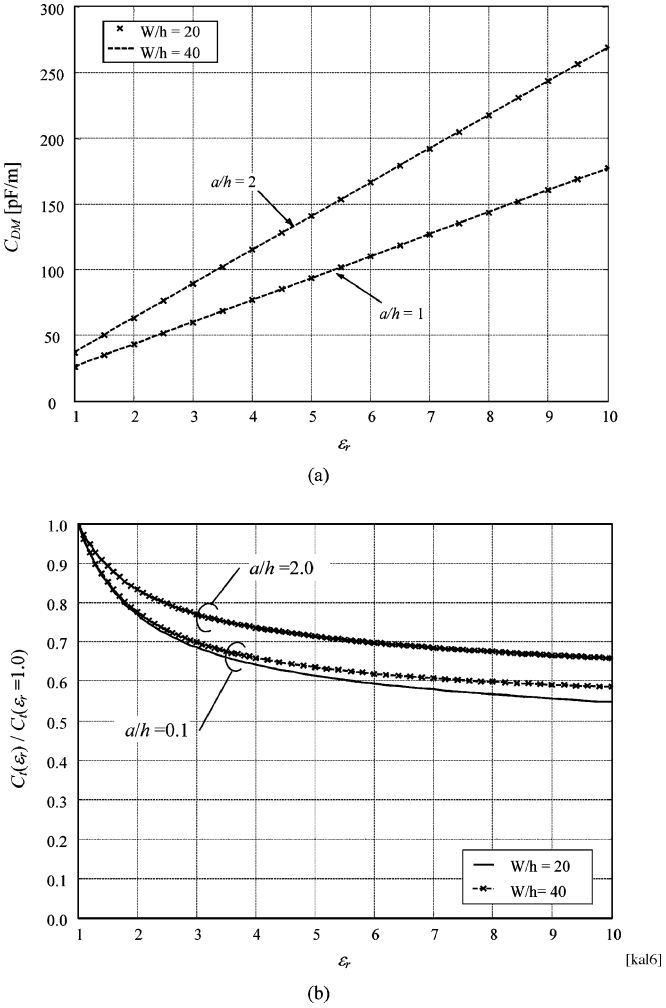

Fig. 5. Calculated capacitances of a microstrip with a finite return plane: (a) mutual capacitance and (b) self-capacitance of the trace.

the dielectric thickness, as shown in Fig. 5(a). The self-capacitance of the trace, C_t, is shown in Fig. 5(b). The capacitance decreases as the relative dielectric constant increases. However, the variation in self-capacitance due to the substrate is less than 40% for relative dielectric constants up to 5.0 for a typical microstrip where the ratio of board width to trace height is 20. The variation is less than 45%, even when the relative dielectric constant is 10. In practice, the variation is even smaller because most PCBs have dielectric constants less than 5.0 and width/height ratios greater than 0.1. For typical board geometries, the variation in the trace self-capacitance due to the dielectric material will generally be less than a few decibels. Considering the approximate nature of most radiated electromagnetic interference estimates, the dielectric permittivity plays a relatively minor role in the calculation of C_t. However, the geometry of the microstrip, such as the width of the return plane and dielectric thickness, has a significant effect.

III. Closed-Form Expression for Estimating Self-Capacitance of a Trace

When the length of the board is much greater than the width, the effects of stray fields at each end of the trace can be taken into account by adding an equivalent stub length to the microstrip. This approach has been used to model the open ends of microstrips [10]. Thus, an equivalent expression for the self-capacitance of a trace may take the following form:

$$C_t = C_{t,\text{pul}} \times (l_t + l_{\text{eq}}) \tag{1}$$

where $C_{t,\text{pul}}$ is the per unit length self-capacitance of the trace, and l_t and l_{eq} are the actual length and equivalent stub length of the microstrip, respectively. However, this expression cannot be used for a board when the length is comparable to the width. Because the length of most PCBs is comparable to the width, 3D simulations of various trace/board geometries were conducted to explore the effects of trace position and aspect ratio of the board on C_t. The closed-form expression for C_t should have the following form:

$$C_t = f(W, L, d_i) \times \frac{Q_{\text{ex}}(W, a, h, l_t)}{V_t} \tag{2}$$

where W and L are the width and length of the board, d_i is distance of the trace from each edge, and Q_{ex} is the available excess charge per unit length in an infinitely long 2-D configuration with a plane width W. To investigate the effects of distance between the trace and the edges of the board, a trace was evaluated at different positions on a board. The self-capacitance was calculated using *FastCap* [11]. The results for a 2-cm-long, 1-mm-wide trace that is located 1 mm above a plane are shown in Fig. 6.

The simulated results show that the distance of the trace from the longitudinal edges (i.e., offset of the trace along the y-axis) has a strong effect on the self-capacitance of the trace, whereas the distance from other edges has little effect. The results are not surprising because most

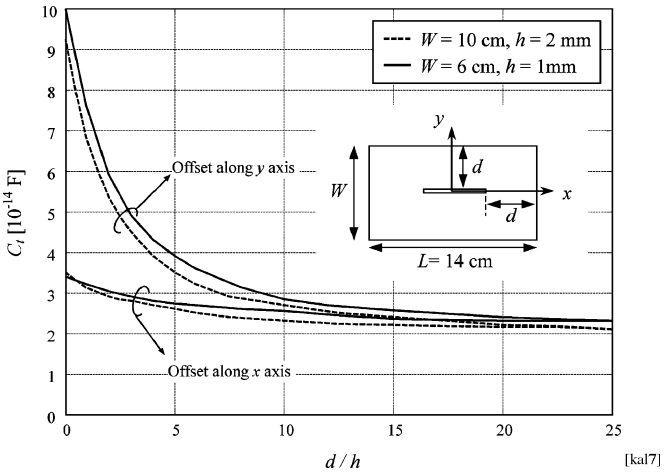

Fig. 6. Trace self-capacitance as a function of position above a finite plane.

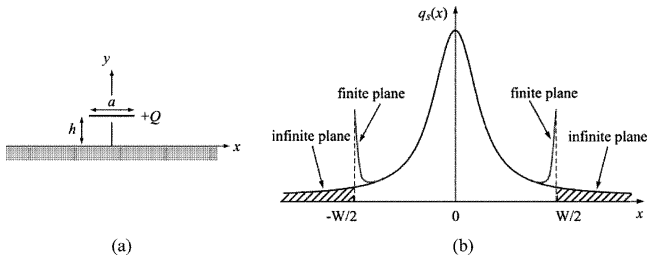

Fig. 7. Charge distributions on return planes: (a) microstrip geometry and (b) charge redistribution due the truncation of return plane.

of the excess charge is induced on the longitudinal edges. An interesting observation is that the capacitance does not change significantly if the trace is located more than ten times the trace height h away from the edge of the board. This implies that the distance between the trace and each edge can be neglected, as long as the trace is not located too near an edge. For traces located away from the edges of the board, (2) can be simplified as

$$C_t = f(W, L) \times \frac{Q_{\rm ex}(W, a, h, l_t)}{V_t}. \tag{3}$$

A. Quantifying Excess Charges

The self-capacitance of the trace is associated with the electric fields terminating at infinity when the potentials at the return plane and infinity are set to 0 V. To express the amount of the charge induced at infinity, a 2D model is used again. Fig. 7 illustrates the geometry considered and the charges induced on the return plane with infinite and finite planes. Due to the truncation of the plane, a portion of the charge induced off the plane is redistributed, resulting in a dense charge distribution at the edges of the plane, as shown in Fig. 7(b). Intuitively, one might expect the total charge induced at infinity to be proportional to the total charge induced over $|x| \geq W/2$ for the infinite plane.

If the potentials are known, the charge distributions on the return plane can be expressed as

$$\sigma_{W=\infty}(x) = \varepsilon_o \frac{\partial}{\partial_y} \phi(x, y)\bigg|_{y=0}. \tag{4}$$

Using the 2D Green's function, the potential at an arbitrary point can be represented as an integral form:

$$\phi(\bar{\rho}) = \int_c G(\bar{\rho}, \bar{\rho}')\sigma(\bar{\rho}')dc' \tag{5}$$

where $G(\bar{\rho}, \bar{\rho}') = -\ln(\bar{\rho} - \bar{\rho}')/2\pi\varepsilon_o$, C represents the conductor contour where the charges are located, and $\bar{\rho}$ and $\bar{\rho}'$ are coordinate vectors representing the observation and source positions, respectively. When the plane width is infinite, image theory can be used, and the potential can be calculated by integrating over the trace and its image. By plugging (5) into (4), the charge distribution on the return plane is given by

$$\sigma_{W=\infty}(x) = \frac{h}{\pi} \int_{-a/2}^{a/2} \frac{\sigma(x')}{(x - x')^2 + h^2}\, dx'. \tag{6}$$

If the charge distribution on the trace is known, the charge distribution on the return plane can be determined from (6). The simplest expression is obtained by assigning a uniform charge distribution to the trace. In this case, the charge on the plane is given by

$$\sigma_{W=\infty}(x) = -\frac{Q}{a\pi}\left[\tan^{-1}\left(\frac{2x + a}{2h}\right) - \tan^{-1}\left(\frac{2x - a}{2h}\right)\right] \tag{7}$$

where Q is total charge on the trace and is approximately $C_{\rm DM}V_t$, where $C_{\rm DM}$ is the capacitance of the trace with an infinitely wide return plane. Note that the dielectric material is not considered in this case. A closed-form expression for $C_{\rm DM}$ can be found in the literature [10], [12] and is given by

$$C_{\rm DM} = 2\pi\varepsilon_o \left\{\ln\left[\frac{F_1 \cdot h}{a} + \sqrt{1 + \left(\frac{2h}{a}\right)^2}\right]\right\}^{-1} \tag{8}$$

where

$$F_1 = 6 + (2\pi - 6)\exp\left\{-\left(30.666 \times \frac{h}{a}\right)^{0.7528}\right\}. \tag{9}$$

Because the charge distribution is assumed to be uniform, (7) works well if $a/h = 1$. The effects of nonuniform charge distribution are investigated by comparing charge distributions on the plane for different widths of the trace. Approximate closed-form expressions for nonuniform charge distributions on the trace are available in the literature [10], [14]. These nonuniform trace distributions were used to calculate the charge distribution on the return plane, and the results are shown in Fig. 8. The results show that the charge distribution on the plane is a little greater directly below the trace for nonuniform trace charge distributions; however, at observation points away from the trace, little difference can be found, and a simple uniform distribution of the trace charge can be used without a significant loss of accuracy. This implies that (7) can be used to calculated the charge at $|x| \geq W/2$, even for a wide trace $(a/h > 1)$, when the board is much wider than the trace (i.e., $W \gg a$).

Using the expression for charge distribution on the plane in (7), the total excess charge on $|x| \geq W/2$ can be expressed as

$$\begin{aligned}
\frac{Q_{\rm ex}}{l_t} &= 2\int_{W/2}^{\infty} \sigma_{W=\infty}(x)\, dx \\
&\approx -\frac{2V_tC_{\rm DM}}{a\pi}\int_{W/2}^{\infty}\left[\tan^{-1}\left(\frac{2x + a}{2h}\right) - \tan^{-1}\left(\frac{2x - a}{2h}\right)\right] dx \\
&\approx -\frac{2V_tC_{\rm DM}}{\pi}\left[\frac{\pi}{2} - \tan^{-1}\left(\frac{W}{2h}\right)\right] \\
&\approx \frac{4hV_tC_{\rm DM}}{\pi W}, \quad \text{for } W \gg h
\end{aligned} \tag{10}$$

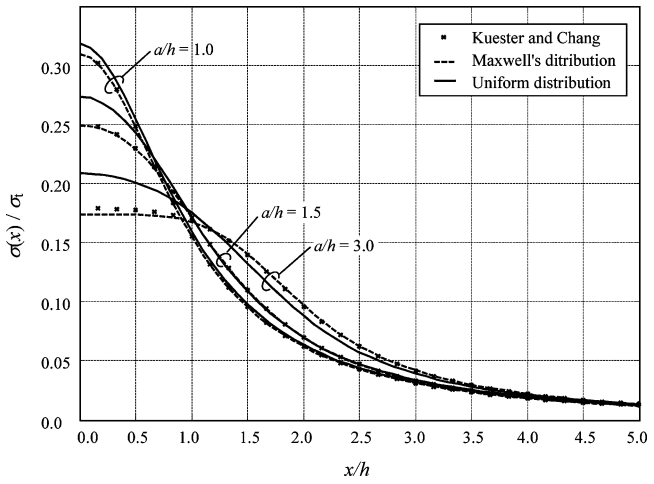

Fig. 8. Charge distributions on infinitely wide return plane with various charge distributions on the trace. $a = h = 1$ mm.

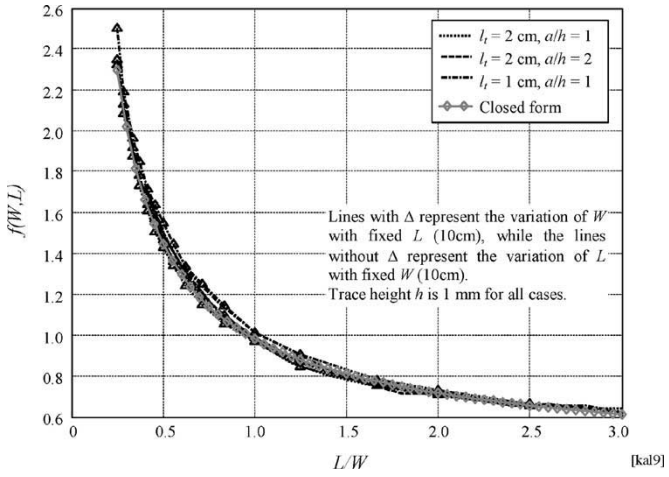

Fig. 9. Effects of board dimensions on the self-capacitance of the trace.

where l_t is the length of the microstrip. Substituting (10) into (3), the self-capacitance of the trace can be rewritten as

$$C_t = f(W, L) \times \frac{4hC_{\mathrm{DM}}l_t}{\pi W}. \tag{11}$$

B. Consideration of Board Dimensions

The effects of board dimensions on C_t are represented by the $f(W, L)$ term in (11). Values of this term were numerically calculated for various geometries using *FastCap*. One set of numerical data is illustrated in Fig. 9. A simple closed-form expression that fits the data collected with the minimum root-mean-square error is given by

$$f(W, L) = \frac{1.547}{\ln\left[1 + 3.845\left(\frac{L}{W}\right)\right]} \tag{12}$$

and is illustrated in Fig. 9. Combining (12) with (11), a closed-form expression for C_t is obtained and is given by

$$C_t = \frac{6.189}{\pi} \cdot \frac{h}{W} \cdot \frac{C_{\mathrm{DM}}l_t}{\ln\left[1 + 3.845\left(\frac{L}{W}\right)\right]}. \tag{13}$$

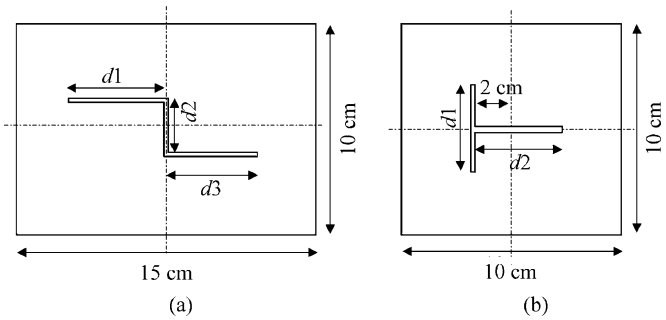

Fig. 10. Configurations of test boards with (a) bent and (b) bifurcated traces.

TABLE 1
COMPARISON OF SELF-CAPACITANCE OF A TRACE

d1 (cm)	d2 (cm)	d3 (cm)	a = h = 1 mm		a = 2 mm, h = 1 mm		a = 1 mm, h = 2 mm		a = h = 2 mm	
			NUM	CF	NUM	CF	NUM	CF	NUM	CF
Bent trace										
4.0	2.0	4.0	2.7	2.72	3.8	4.25	4.1	4.53	5.4	5.98
4.0	2.0	2.0	2.1	2.18	3.0	3.48	3.2	3.71	4.2	4.89
2.0	2.0	2.0	1.5	1.63	2.3	2.70	2.3	2.89	3.2	3.81
Bifurcated trace										
4.0	5.0	3.0	2.96		4.2	4.21	4.4	4.50	5.7	5.93
0.0	5.0	1.7	1.64		2.4	2.34	2.5	2.50	3.3	3.29
4.0	0.0	1.3	1.32		2.0	1.87	2.06	2.00	2.7	2.63

Unit: 10^{-14} F.

NUM, numerical data; CF, closed-form expression.

IV. Evaluation of Closed-Form Expression

To evaluate the effectiveness of the derived closed-form expression for the trace self-capacitance, boards with various trace and plane geometries were analyzed. Numerically calculated capacitances were compared with the closed-form results (13). For all configurations, the trace was located away from the edges of the board so the distance between the trace and the edges was at least ten times greater than the trace height. Two of the test boards are illustrated in Fig. 10. The self-capacitance of the trace was calculated for various lengths of each segment.

Table I shows the calculated capacitances. Total closed-form capacitances were obtained by summing the contribution of each segment. Numerical values were calculated using *FastCap*. For all configurations evaluated, the error was less than 20% (<2 dB). The results also show that the greater the offset of the trace from the edges, the smaller the error. This level of accuracy is generally more than sufficient for estimating the common-mode current on attached cables.

V. Conclusion

A closed-form expression for estimating the self-capacitance of a PCB trace, C_t, above a solid plane was derived. The value of C_t was found to be relatively independent of the dielectric permittivity of the substrate for typical configurations. The derived expression can be used for traces that are located away from the edges of the board by at least ten times the height above the plane. For the tested configurations, this expression provided capacitance values within 20% of the values obtained from a 3-D static field modeling code.

The derived closed-form expression in this article can be used to estimate the voltage-driven common-mode current due to microstrip traces on PCBs [6]. Using the closed-form expression, calculations can be performed more quickly and easily than they can be using a field modeling code. The closed-form expression also provides insight regarding the effects that various geometric parameters have on the voltage-driven emissions from PCBs.

REFERENCES

[1] D. Hockanson, J. Drewniak, T. Hubing, T. Van Doren, F. Sha, and M. Wilhelm, "Investigation of fundamental EMI source mechanisms driving common-mode radiation from printed circuit boards with attached cables," *IEEE Trans. Electromagn. Compat.*, vol. 38, no. 4, pp. 557–566, Nov. 1996.

[2] D. Hockanson, J. Drewniak, T. Hubing, T. Van Doren, F. Sha, C. W. Lam, and L. Rubin, "Quantifying EMI resulting from finite-impedance reference planes," *IEEE Trans. Electromagn. Compat.*, vol. 30, no. 4, pp. 286–297, Nov. 1997.

[3] M. Leone, "Design expressions for trace-to-edge common-mode inductance of a printed circuit board," *IEEE Trans. Electromagn. Compat.*, vol. 43, no. 4, pp. 667–671.

[4] G. Dash, J. Curtis, and I. Straus, "The current driven model—Experimental verification and the contribution of I_{dd} delta to digital device radiation," in *Proc. 1999 IEEE Int. Symp. Electromagn. Compat.*, Seattle, WA, Aug. 1999, pp. 317–322.

[5] R. Dockey and R. German, "New techniques for reducing printed circuit board common-mode radiation," in *Proc. 1993 IEEE Int. Symp. Electromagn. Compat.*, Dallas, TX, Aug. 1993, pp. 334–339.

[6] H. W. Shim and T. H. Hubing, "Model for estimating radiated emissions from a printed circuit board with attached cables driven by voltage-driven sources," *IEEE Trans. Electromag. Compatibility*, vol. 47, no. 4, pp. 899–907, Nov. 2005.

[7] C. Smith and R. Chang, "Microstrip transmission line with finite-width dielectric and ground plane," *IEEE Trans. Microw. Theory Tech.*, vol. 33, no. 9, pp. 835–839, Sep. 1985.

[8] C. Smith and R. Chang, "Microstrip transmission line with finite-width dielectric," *IEEE Trans. Microw. Theory Tech.*, vol. 28, no. 2, pp. 90–94, Feb. 1980.

[9] R. F. Harrington, K. Pontoppidan, P. Abrahamsen, and N. C. Albertsen, "Computation of Laplacian potentials by an equivalent source method," *Proc.*, vol. 116, no. 10, pp. 1715–1720, Oct. 1969.

[10] K. C. Gupta, R. Garg, and I. Bahl, *Microstrips and Slot Lines*, 2nd ed. Norwood, MA: Artech House, 1996.

[11] K. Nabors, S. Kim, J. White, and S. Senturia, *FastCap User's Guide. Cambridge: Research Laboratory of Electronics, Department of Electrical Engineering and Computer Science,* Massachusetts Institute of Technology, Cambridge, 1992.

[12] F. Schnieder and W. Heinrich, "Model of thin-film microstrip for circuit design," *IEEE Trans. Microw. Theory Tech.*, vol. 49, no. 1, pp. 104–110, Jan. 2001.

[13] E. F. Kuester and D. C. Chang, "Closed-form expressions for the current or charge distribution on parallel strips or microstrip," *IEEE Trans. Microw. Theory Tech.*, vol. 28, no. 3, pp. 254–259, Mar. 1980.

[14] M. Kobayashi, "Longitudinal and transverse current distributions on microstrips and their closed-form expression," *IEEE Trans. Microw. Theory Tech.*, vol. MTT-33, no. 9, pp. 784–788, Sep. 1985.

Long Range Propagation of Lightning Pulses Using the FDTD Method

Jean-Pierre Bérenger

***Abstract*—The numerical dispersion of the finite-difference time-domain (FDTD) method is a serious drawback in view of computing long range propagation of lightning pulses in the Earth-ionosphere waveguide. In this paper, it is shown that most of this dispersion can be removed by postprocessing the FDTD results. This makes possible the propagation of lightning pulses up to thousands of kilometres with reasonable computational times.**

***Index Terms*—Finite difference, finite-difference time-domain (FDTD), low frequency (LF), lightning, propagation, very low frequency (VLF).**

I. INTRODUCTION

In recent years, the finite-difference time-domain (FDTD) method [1], and [2], has been applied to the propagation of waves in the Earth-ionosphere waveguide at frequencies ranging from extreme low frequency (ELF) to low frequency (LF). This numerical technique is used in [3] and [4] for predicting VLF-LF radio links in a frequency band from 15 to 70 kHz. In [5], it is applied to the propagation of ELF-VLF lightning pulses over a 1000 km ground path. Finally, as discussed in [6] and [7], it allows the propagation of ELF waves to be computed around the entire Earth.

In this paper, it is shown that the FDTD method can also be used for propagating lightning pulses over paths of several thousands kilometres in length. From this, the contribution of lightning to the natural noise can be computed up to large distances from the lightning location. This will permit the FDTD method to be used in further investigations of the natural noise in the frequency band of interest for VLF-LF communications.

Numerical dispersion, which is a general drawback to the FDTD method [1], is emphasized in VLF-LF propagation because the ratio of the path length to the wavelength is quite large at the frequencies of interest. From this, time domain pulses are strongly distorted as they propagate in the FDTD grid. It is shown that this drawback can be widely reduced by means of a simple method that consists of post-processing the FDTD results as if the propagation were one-dimensional. This allows the propagation of lightning pulses to be computed up to distances larger than 5000 km with reasonable FDTD cell sizes; i.e., with reasonable computational times.

II. THE FDTD METHOD FOR COMPUTING PROPAGATION OF PULSES IN THE EARTH-IONOSPHERE WAVEGUIDE

The computational code used in this paper has been described in detail in [3] and [4] for the propagation of radio waves. Only minor changes have been introduced to account for the time domain aspect of the pulse that replaces the sinusoidal wave.

Maxwell's equations are solved in a two-dimensional system of spherical coordinates whose origin is the center of the Earth. The FDTD scheme [4] can account for the natural magnetic field. This scheme is basically a second order Yee scheme [1], with the adjunction of an auxiliary differential equation within the anisotropic ionosphere [4].

As with radio waves, Maxwell's equations are solved only within a moving domain (Fig. 1) so as to reduce the computational time. Some changes have been introduced to the settings of this domain. First, its

Manuscript received August 6, 2003; revised October 19, 2004.

The author is with the Centre d'analyse de Defense, 94114 Arcueil Cedex, France (e-mail: berenger@cad.etca.fr).

Digital Object Identifier 10.1109/TEMC.2005.858747